Appl. Phys. B 75, 53–58 (2002)
DOI: 10.1007/s00340-002-0945-1

Applied Physics B
Lasers and Optics

P.L. RAMAZZA[1,2,✉]
S. DUCCI[3]
A. ZAVATTA[1,4]
M. BELLINI[1,2]
F.T. ARECCHI[1,2,5]

Second-harmonic generation from a picosecond Ti:Sa laser in LBO: conversion efficiency and spatial properties

[1] Istituto Nazionale di Ottica Applicata, 50 125 Florence, Italy
[2] INFM, Sezione di Firenze, 50 125 Florence, Italy
[3] Ecole Normale Supérieure de Cachan, 94 235 Cachan Cedex, France
[4] Dipartimento di Sistemi e Informatica, Universitá di Firenze, Italy
[5] Dipartimento di Fisica, Universitá di Firenze, Italy

Received: 13 March 2002/Revised version: 8 May 2002
Published online: 12 July 2002 •

ABSTRACT We report an experimental study of the second harmonic generated in type I interaction by a Ti:Sa laser operating in the picosecond regime at 786 nm in LBO crystals. A joint characterization of the dependence of conversion efficiency and spatial beam quality on crystal length and degree of pump focusing is given. A simple heuristic formula, reproducing over a broad range of parameters the predictions of classical Boyd–Kleinman theory, is derived and compared with the experimental results. The conditions for the optimization of the generation process using an elliptically focused pump beam are quantitatively evaluated.

PACS 42.65.-k; 42.70.-a

1 Introduction

Among the nonlinear crystals available for harmonic generation from visible and near-IR lasers, LBO has received particular attention due to its large nonlinearity, broad wavelength tunability, and wide transmission region [1–3]. Besides these fundamental characteristics, LBO also displays a high damage threshold, optical homogeneity, and a wide temperature bandwidth, features that increase its attractiveness in experiments.

Second-harmonic generation (SHG) in LBO has been studied in several experimental setups. Investigations of this phenomenon in single-pass geometry [4–10], in intracavity configuration [11], and in a resonant cavity external to the pump laser [12–15] are reported in the literature.

In most of these studies, either the crystal length is fixed or the focusing parameter is held constant at the value which maximizes the generation efficiency. This value is evaluated on the basis of the classical theory of Boyd and Kleinman (B-K) [16] for the SHG generated using focused Gaussian beams. The issue of transverse beam quality has been seldom addressed. In very few cases [14] the value of the quality factor M^2 of the beam generated at the experimental parameters giving the maximum efficiency has been given. However, a systematic report of the dependence of the generated beam shape on the experimental parameters is not available for this crystal in the literature.

In this paper we report an experimental study of the efficiency and of the spatial properties of the second harmonic generated by a Ti:Sa laser operating in the ps regime in LBO. Using a single-pass geometry, we investigate the dependence of the generation efficiency on the crystal length and the focusing parameter. We compare the results with the prediction of the B-K theory, and we introduce a simplified heuristic treatment that retains the basic physical phenomena involved in the SHG process. The limits of validity of this approach are discussed, showing that its predictions are applicable to many cases of experimental interest. We therefore propose the results of this treatment as a simple tool that can be used for quick evaluation of a given crystal performance in SHG, and for the optimization of the process by a choice of the appropriate crystal type and laboratory parameters.

Besides the efficiency measurements, we show the variation of the generated beam profile with the crystal length and the focusing parameter.

Joint information on the two above aspects is of great importance for several applications, in which the generated light is to be, for example, coupled to an optical cavity or refocused to generate other nonlinear effects. Finally, we evaluate quantitatively the possibility of increasing the generation efficiency using an elliptical rather than a spherical focusing of the pump beam.

2 Efficiency of the second-harmonic generation: Boyd–Kleinman theory and simplified approach

The theory of second-harmonic generation with focused Gaussian beams has been developed in a classical paper [16], in which an expression for the efficiency conversion as a function of the most important experimental parameters is given. Here we briefly recall the results of this theory. Let us consider a Gaussian pump beam described by the electric field

$$E = \frac{E_0 \mathrm{e}^{\mathrm{i}k_1 z}}{1+\mathrm{i}\tau} \exp\left(-\left(x^2+y^2\right)/\left(w_0{}^2(1+\mathrm{i}\tau)\right)\right) \quad (1)$$

focused at the center of a nonabsorbing crystal. According to the usual notation, k_1 is the longitudinal wavenumber of the light at the fundamental frequency $\omega = k_1 c/n_1$ propagating in a crystal of refractive index n_1. The beam has radius w_0 at

✉ Fax: +39-055/233-7755, E-mail: pier@ino.it

its waist, which is assumed to be located in the central plane $z = l/2$ of the crystal of length l. The factor $\tau \equiv (2z - l)/b$, where $b \equiv {w_0}^2 k_1$ is the confocal parameter, describes the evolution of the beam size and wavefront curvature in the course of propagation, following the usual Gaussian-beam theory. In these conditions, the B-K calculations predict for the generation of light at the second-harmonic frequency 2ω, with wavenumber $k_2 = 2\omega n_2/c$, a conversion efficiency

$$\eta \equiv \frac{P_{2\omega}}{P_\omega} = K P_\omega l k_1 h(\sigma, B, \xi) \,. \tag{2}$$

Here

$$K = \frac{2\omega^2 {d_{\text{eff}}}^2}{\varepsilon_0 {n_1}^2 n_2 c^3 \pi} \,, \tag{3}$$

where d_{eff} (pm/V) is the effective second-order polarization coefficient of the crystal, P_ω, $P_{2\omega}$ are the powers of the pump and generated beams, and the function $h(\sigma, \beta, \xi)$ is defined as

$$h(\sigma, B, \xi) = \frac{1}{4\xi} \int_{-\xi}^{\xi} \int_{-\xi}^{\xi} \frac{\mathrm{e}^{\mathrm{i}\sigma(\tau-\tau')} \mathrm{e}^{-B^2(\tau-\tau')^2/\xi}}{(1+\mathrm{i}\tau)(1-\mathrm{i}\tau')} \mathrm{d}\tau \mathrm{d}\tau' \,. \tag{4}$$

This function weights the contributions to the harmonic power arising at different longitudinal locations inside the crystal.

The quantities upon which h depends are the focusing parameter $\xi \equiv l/b$, the normalized mismatch $\sigma \equiv b\Delta k/2$, with $\Delta k \equiv \mid 2k_1 - k_2 \mid$, and the nondimensional walk-off parameter B, defined as $B \equiv (\varrho/2)\sqrt{lk_1}$ for a crystal having a walk-off angle ϱ. The above results hold for type I three-wave interactions, which typically give higher efficiencies with respect to type II ones. In the following we will refer to type I interactions.

It is practically always of interest to optimize the SHG efficiency with respect to the mismatch parameter σ. For this purpose the function

$$h_{\text{m}}(B, \xi) \equiv \max[h(\sigma, \beta, \xi)]_\sigma \tag{5}$$

is used instead of (4). We refer to this function in the rest of the paper, when comparing the prediction of the B-K theory with experimental results and with the expectations based on our simplified treatment of the SHG process.

The reason for giving here this simplified approach to the evaluation of the SHG efficiency is twofold. On one hand, we wish to offer a self-contained paper, by briefly reviewing the role of the physical mechanism that limits the conversion efficiency; on the other hand, our endpoint is a very simple formula, which can be used for fast, but still rather precise, evaluation of crystal performances in generating second-harmonic radiation.

Let us consider as a starting point an unfocused Gaussian beam of waist w_0 impinging on a crystal of length l, at the correct angle for phase-matched second-harmonic generation. By 'unfocused beam' we mean here that the beam confocal parameter is much larger than the crystal length. In the absence of walk-off, the efficiency of the SHG process is given by the plane-wave expression [17]

$$\eta = K \frac{P_\omega}{{w_0}^2} l^2 \,, \tag{6}$$

with K defined in (3). This expression, easily derivable for cw laser beams, is also valid for pulsed sources, provided that the crystal length is smaller than

(i) the characteristic length over which the pump pulse broadens due to dispersion; this length is given by $l_{\text{disp}} = \tau^2/g$, where g represents the group-velocity dispersion, and is of the order of several meters when operating in the ps pulsed regime,

(ii) the longitudinal walk-off length, often referred to as the 'quasistatic length', which is $l_{\text{qs}} = \tau\nu^{-1}$ [18], with $\nu \equiv {v_{\text{g}_1}}^{-1} - {v_{\text{g}_2}}^{-1}$, v_{g_1}, v_{g_2} being the group velocities of the light at the fundamental and harmonic frequencies. This length is of the order of centimeters for the crystals and pulses considered here (see Sect. 3).

The simultaneous fulfilment of the above conditions about the crystal length ensures the absence of broadening of the pump and of the generated second-harmonic pulses.

In the presence of transverse walk-off due to birefringence, the pump and second-harmonic-generated beams separate spatially while propagating through the crystal. After a distance $l_{\text{a}} \simeq w_0/\varrho$ the two beams are no longer overlapped in the transverse plane; hence the coherence of the generation process along the propagation direction is lost. The rigorous analysis of B-K gives $l_{\text{a}} = \pi^{1/2} w_0/\varrho$, and we will adopt this definition in the following. Since l_{a}, often called the aperture length, poses a limit to the length of coherent interaction along the propagation direction, the generation efficiency in the presence of walk-off is no longer given by (6), but by a sum of 'micro-efficiencies' of the same form over the number $N = l/l_{\text{c}}$ of coherent interaction lengths l_{c}. In the asymptotic cases, $l_{\text{c}} = l$ for $l_{\text{a}} >> l$ and $l_{\text{c}} = l_{\text{a}}$ for $l_{\text{a}} << l$. As a tentative function to reproduce the dependence of l_{c} on l_{a} also at intermediate values of l_{a}, we introduce $l_{\text{c}} = l \tanh(l_{\text{a}}/l)$. Using this expression and summing over the N coherence lengths, we obtain

$$\eta = K \frac{P_\omega}{{w_0}^2} l^2 \tanh\left(\frac{l_{\text{a}}}{l}\right) \,. \tag{7}$$

Next, we consider the effect of pump beam focusing. We limit our considerations to the case in which the pump is focused at the center of the crystal. The term $P_\omega/{w_0}^2$ in (7) represents the pump intensity, and propagates along z according to the usual Gaussian-beam rules. The average value of the pump intensity along the propagation direction is therefore

$$\begin{aligned} \langle I(z) \rangle_z &\equiv \frac{1}{l} \int_{-l/2}^{l/2} I(z) \mathrm{d}z \\ &= \frac{1}{l} \frac{P_\omega}{{w_0}^2} \int_{-l/2}^{l/2} \frac{\mathrm{d}z}{1 + 4z^2/b^2} = \frac{P_\omega}{{w_0}^2} \frac{b}{l} \operatorname{atan}\left(\frac{l}{b}\right) \,. \end{aligned} \tag{8}$$

This means that the average intensity is given by a fraction $\beta \equiv (b/l)\text{atan}(l/b)$ of the maximum intensity $P_\omega/{w_0}^2$. This fraction is $\simeq 1$ for $b >> l$, and $\simeq b/l$ for $b << l$. The usual way to interpret this result is that SHG will actually be very efficient not along the whole crystal length, but only along a fraction β of it over which the input intensity maintains approximately its maximum value.

In order to take into account that for values of the focusing parameter $\xi \gtrsim 1$ the pump intensity, to which the conversion efficiency is proportional, is not constant along the crystal, we substitute $P_\omega/{w_0}^2$ in (7) with its average value given by (8); we obtain

$$\eta = K\frac{P_\omega}{{w_0}^2}l^2\frac{b}{l}\text{atan}\left(\frac{l}{b}\right)\tanh\left(\frac{l_\text{a}}{l}\right), \tag{9}$$

which is our estimation of the SHG efficiency taking into account the effects of walk-off and focusing. Recalling that $\xi \equiv l/b$, (9) can be cast in a form more directly comparable with the Boyd–Kleinman formula (2) for the generated power:

$$\eta = KP_\omega l k_1 \text{atan}(\xi)\tanh\left(\frac{\pi^{1/2}}{2B}\frac{1}{\xi^{1/2}}\right). \tag{10}$$

In order to draw a parallel between the predictions of our simplified approach and the ones of the Boyd–Kleinman theory, it is therefore necessary to compare the function $h_\text{m}(B, \xi)$ defined in (5) with the function

$$g(B, \xi) \equiv \text{atan}(\xi)\tanh\left(\frac{\pi^{1/2}}{2}\frac{1}{B\xi^{1/2}}\right). \tag{11}$$

We start by noticing that in the case of weak focusing the function g has exactly the same asymptotic behavior as that reported for the function h_m in [16], namely

$$g(B, \xi) \simeq \xi \quad \text{for} \quad \xi << 1,\ \xi << \frac{1}{B^2}, \tag{12}$$

$$g(B, \xi) \simeq \frac{\pi^{1/2}}{2}\frac{\xi^{1/2}}{B} \quad \text{for} \quad \xi << 1,\ \xi >> \frac{1}{B^2}. \tag{13}$$

At intermediate values of focusing strength, we have instead

$$g(B, \xi) \simeq \text{atan}(\xi)\,\frac{\pi^{1/2}}{2}\frac{1}{B\xi^{1/2}} \quad \text{for} \quad \xi \simeq 1,\ \xi >> \frac{1}{B^2}. \tag{14}$$

This formula also coincides with the one given in [16] in this range of parameters. The validity of (11) is limited at upper values of ξ, however. This limit can be understood by going back to the very strong hypothesis that we have implicitly introduced in our derivation of $g(B, \xi)$. The hypothesis consists in considering the effects of walk-off and of diffraction as acting separately. More specifically, we have considered the crystal as a succession of coherent segments, all of which have the same length l_a (for $l_\text{a} << l$), and we have subsequently averaged the intensity distribution that varies along the crystal due to diffraction. This procedure implicitly requires that the focal depth b is considerably larger than the aperture length l_a. Hence, we expect that our derivation gives acceptable results for values of the focusing parameter ξ such that $l_\text{a} \lesssim b$. This sets the limiting value $\xi \lesssim \xi_\text{c} \equiv 4B^2/\pi$, which defines the upper limit to the range of validity of (11). According to the above discussion, this limit applies only if $\xi \geq 1$; in the opposite case diffraction is inefficient on the crystal length scale, and our derivation takes correctly into account the role of walk-off in affecting the SHG efficiency. Hence, the overall range of validity expected for g is $\xi \lesssim \max[1, \xi_\text{c}]$.

In Fig. 1 we report a comparison between $g(B, \xi)$ and the function $h_\text{m}(\beta, \xi)$ given by the B-K theory. The shadowed region is defined by $\xi > \xi_\text{c}$ at $\xi > 1$, and represents the part of the parameter space in which agreement between g and h_m is not expected. It is seen here that the agreement between the two functions is good over all the range of validity of the approximations we have used, and not only in the above-discussed asymptotic regimes. It is worth noticing that our function g is obtained by assuming that all the plane-wave components of the Gaussian beam are phase-matched, so that no optimization with respect to a phase-matching parameter is required. This does not lead to strong discrepancies between g and h_m for crystals with moderate or large walk-off $B \gtrsim 1$, as in this case the optimal phase matching differs very little from the ordinary one [16].

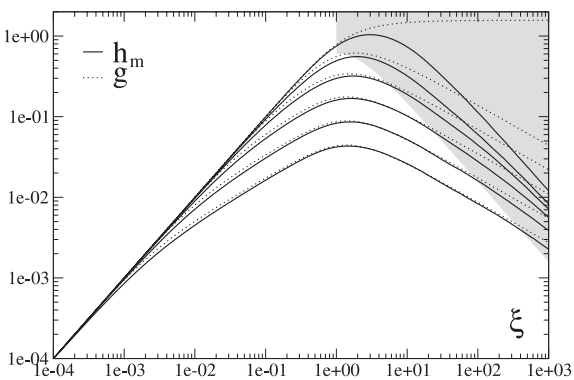

FIGURE 1 Comparison between the Boyd–Kleinman function $h_\text{m}(\xi)$ (*continuous lines*) and the function $g(\xi)$ given by our simplified approach (*dashed lines*), for several values of the walk-off parameter B. *Top to bottom curves*: $B = 0$, 1, 2, 4, 8, 16. In the *grey region* the approximations leading to the evaluation of g are not valid

We do not attempt to extend our approach to the regime in which the diffractive length b is comparable to or shorter than the aperture length l_a, because it corresponds to both a decrease in SHG efficiency and a deterioration of the beam quality with respect to the range of parameters that we are considering, and is usually of little practical interest.

Once the limits of validity of our approach are clarified, therefore, it is possible to use the function g for the estimation of the SHG efficiency, being confident to obtain practically the same results as using the function h_m given by Boyd and Kleinman. In this way it is necessary only to evaluate a simple function of a single variable ξ, instead of having to perform a two-dimensional integral plus a maximization procedure on σ, as required to obtain h_m. This leads to a valuable simplification of the evaluation of a given crystal performance in SHG.

3 Experimental results: efficiencies and beam profiles

Our experimental investigations of second-harmonic generation in LBO are carried out using a Ti:Sa laser operating in the mode-locked regime (Spectra Physics, model Tsunami). In the conditions of the measurements reported here, the laser operates at a wavelength of $\lambda = 786$ nm, with pulses of FWHM duration $\tau = 3$ ps, at a repetition rate $R = 82$ MHz. The beam waist is 0.9 mm (HW at $1/e^2$ of maximum), the divergence is 0.6 mrad full angle, and the cw power is 0.315 W. The second harmonic of this red light is generated by means of type I interaction in the XY crystallographic plane of LBO samples cut at $\theta = 90°$, $\varphi = 33°$, and antireflection-coated at both the red and the blue wavelengths on the input and output faces. As discussed in Sect. 2, longitudinal walk-off of the pump and second-harmonic pulses poses an upper limit to the useful crystal length; this limit is given by the so-called quasistatic length $l_{\rm qs}$. For the pulses of 3 ps in LBO in the conditions of our experiment, $l_{\rm qs} \simeq 23$ mm. The three samples we use are 9-, 13-, and 17-mm long. Since the walk-off angle ϱ is approximately 17 mrad, this corresponds to values of the parameter B equal to 2.88, 3.46, and 3.96.

In Fig. 2 we show the efficiencies measured for the three samples as a function of the pump beam waist (lower), together with the transverse profiles of the generated beam at the exit of the crystal and in the far field (upper). The efficiency data are in excellent agreement with the predictions of our simplified formula (9). We notice here that the expression $\xi \lesssim 4B^2/\pi$, giving the limit of validity of our function $g(\xi)$, can be expressed in dimensional form as $w_0 \gtrsim \lambda/(\sqrt{\pi}2n\varrho)$. Using the LBO parameters, we obtain $w_0 \gtrsim 8$ μm as a regime in which the functions $h_{\rm m}$ and g are practically equivalent. Since all our measurement values of w_0 fall well within this range, we do not report the curves corresponding to the B-K theory in Fig. 2. By comparing the efficiency curves with the spatial beam profiles, it is seen that focusing more tightly than we did leads simultaneously to a worsening of both efficiency and beam quality.

The value of P_ω used to obtain these curves is related to the average laser power $P_{\rm ave}$ by $P_\omega = P_{\rm ave}/3D$, where $D \equiv R\tau$ is the laser duty cycle, and the factor arises when taking into account the sech^2 shape of the laser pulses in the evaluation of the relation between instantaneous and average intensities. The continuous curves in Fig. 2 are obtained for a value of $d_{\rm eff} = 0.683$ pm/V, in good agreement with the data reported in the literature [19].

Concerning the transverse features of the generated beam, relevant information can be grasped from the visual inspection of the beam profiles in Fig. 2. According to the foregoing analysis, three distinct regimes occur in crystals with moderate or large walk-off parameter B when progressively decreasing the pump size w_0. At large values of w_0, namely $w_0 \geq w_{0\varrho} \equiv \varrho l/\pi^{1/2}$, neither walk-off nor diffraction plays a relevant role, and the generated beam reproduces well the Gaussian profile of the pump. For our crystals of lengths 9, 13,

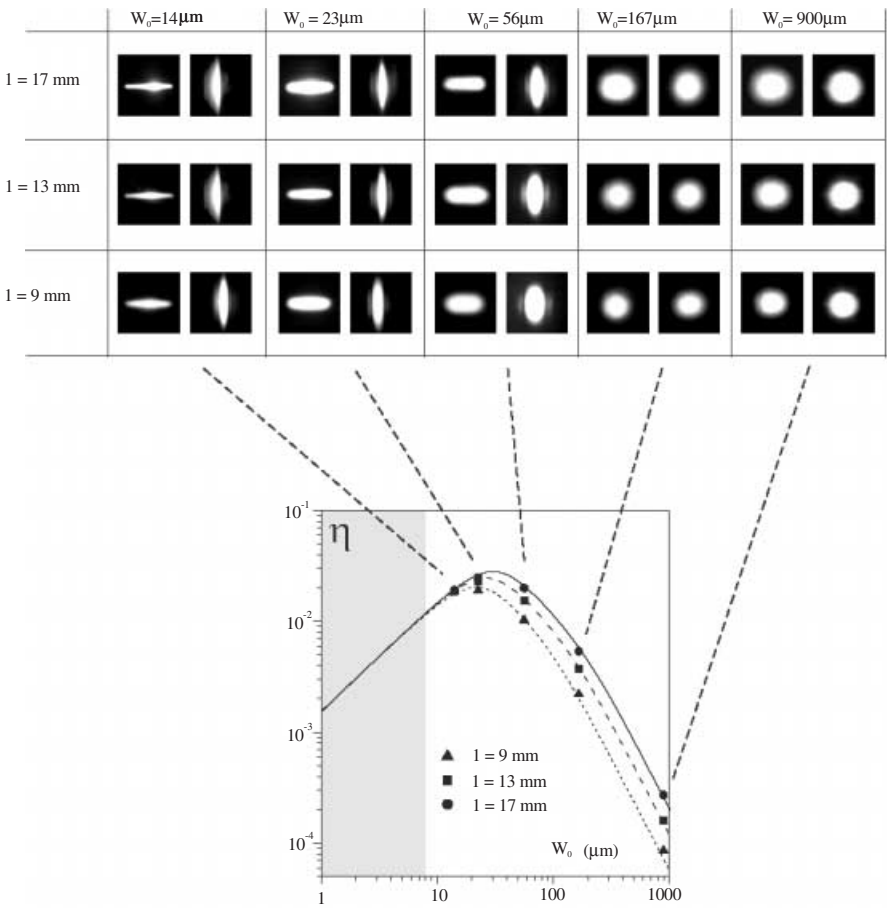

FIGURE 2 *Upper*: spatial distributions of the generated light for the three LBO samples. Inside each frame of the *upper part* of the figure, the beam shapes observed at the crystal exit and in the far field are plotted at *left* and *right*, respectively. The pictures are overexposed in order to allow visualization of low-intensity features. The walk-off direction of the crystal is horizontal. *Lower*: second harmonic generation efficiencies for the three samples. The *points* represent experimental values; the *lines* show the values predicted by our simplified formula (10). The *grey region* is the one in which agreement between the results of our approach and that of B-K theory is not expected (see text)

and 17 mm the values of w_{0_ϱ} are about 86, 125, and 163 μm respectively. Figure 2 shows the regular Gaussian profiles of the generated beams both in the near field and in the far field in this range of w_0.

At intermediate values of w_0, specifically for $w_{0\mathrm{d}} \lesssim w_0 \lesssim w_{0_\varrho}$, where $w_{0\mathrm{d}} \equiv \sqrt{\lambda l/2\pi n}$, diffraction still plays a negligible role, but walk-off is effective. At the output plane of the crystal one observes for the generated beam an elongated shape, resulting from the superposition of the contributions generated at different longitudinal positions inside the crystal. This condition occurs for 26 μm $\leq w_0 \leq$ 86 μm in the shortest crystal, 32 μm $\leq w_0 \leq$ 140 μm in the intermediate one, and 36 μm $\leq w_0 \leq$ 170 μm in the longest one. Correspondingly, in the far field we see the appearance of secondary lobes along the walk-off direction. These lobes are quite symmetric in location and intensity with respect to the central one, and correspond to directions in which the fundamental and harmonic fields are phase-mismatched by an amount $\Delta kl = 2\pi n$, with n an integer. In the range of parameters specified above, the fraction of the total beam energy contained in the central lobe is always larger than 95%.

At even smaller values of w_0 the focusing parameter ξ becomes $\gtrsim 1$, so that both walk-off and diffraction affect the spatial distribution of the generated light. In these conditions, the near-field distribution is not only elongated in the walk-off direction, but also presents a more or less localized thickening in the direction orthogonal to walk-off, resulting in the 'UFO shape' visible in Fig. 2. We can consider as before this intensity distribution as the sum of contributions generated at different longitudinal locations inside the crystal. Now, however, these contributions are very unequal in strength, reflecting the nonuniform profile of the pump beam due to diffraction. The strongest contributions, arising from the focal region, give rise to the thickening observed at the output. As for the far-field profiles, the symmetric lobes observed at intermediate values of w_0 are now replaced by an asymmetric structure in the walk-off direction. This follows from the fact that, for directions forming an angle θ with the crystal x axis smaller than the collinear phase-matching angle θ_{pm}, vectorial phase matching is possible, leading to the generation of light over a broad, continuous range of angles [16]. For θ larger than θ_{pm}, on the contrary, this phenomenon is not possible, and we observe only a set of very low intensity discrete lobes, analogous to the ones reported at intermediate values of w_0. A formal analysis of this strong-focusing regime, giving a full explanation of this kind of spatial structure, is given in [20].

4 Optimization of the conversion efficiency using asymmetric focusing

It has been suggested that in crystals displaying strong walk-off an optimization of the second harmonic generation efficiency can be obtained by the use of asymmetric focusing of the input beam [21, 22]. The idea at the basis of this proposal is to maximize the efficiency by tightly focusing the light in the direction perpendicular to walk-off, thus obtaining a high input intensity, and to use a looser focusing in the walk-off direction, in order to maintain the spatial superposition of the fundamental and harmonic beams over a long distance in the crystal.

Let us consider an elliptical beam of size w_{0x} along the walk-off direction x and w_{0y} in the perpendicular direction. The expression for the second harmonic generation efficiency predicted by the Boyd–Kleinman theory is still given by (2), where now the function h has the form [22]

$$h(\sigma, \beta, \xi_x, \xi_y) = \frac{{\xi_x}^{-3/2}{\xi_y}^{1/2}}{4} \times \int_{-\xi_x}^{\xi_x}\int_{-\xi_x}^{\xi_x} \frac{\mathrm{e}^{\mathrm{i}\sigma(\tau-\tau')}\mathrm{e}^{-B^2(\tau-\tau')^2/\xi_x}\,\mathrm{d}\tau\,\mathrm{d}\tau'}{\sqrt{1+\mathrm{i}\tau'}\sqrt{1+\mathrm{i}\frac{\xi_y}{\xi_x}\tau'}\sqrt{1-\mathrm{i}\tau}\sqrt{1-\mathrm{i}\frac{\xi_y}{\xi_x}\tau}}\,, \quad (15)$$

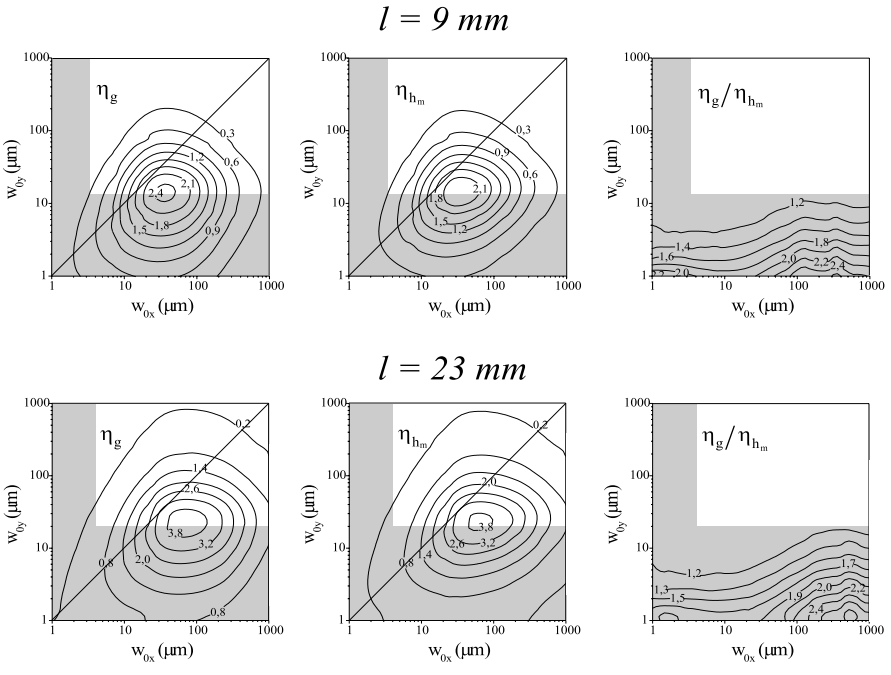

FIGURE 3 Evaluation of the second harmonic generation efficiencies in the case of elliptical focusing. *Left-hand column*: efficiency η_g evaluated using our simplified formulas; *center column*: efficiency $\eta_{h\mathrm{m}}$ evaluated following B-K theory; *right-hand column*: ratio $\eta_g/\eta_{h\mathrm{m}}$. In the *grey regions* agreement between the values of η_g and $\eta_{h\mathrm{m}}$ is not expected (see text)

where $\xi_{x,y} \equiv l/b_{x,y}$ are the values of the focusing parameter along the walk-off direction and the orthogonal one. As in Sect. 2, maximization of h on the detuning σ gives an optimum function h_m. In deriving the simplified function g that we have introduced in Sect. 2, it is now not possible to evaluate analytically the average value of the intensity along the propagation direction. The function g takes the form

$$g(B,\xi_x,\xi_y) = \frac{1}{2}\frac{{\xi_y}^{1/2}}{{\xi_x}^{1/2}} \tanh\left(\frac{\pi^{1/2}}{2}\frac{1}{B{\xi_x}^{1/2}}\right) \times \int_{-\xi_x}^{\xi_x} \frac{\mathrm{d}\tau}{\sqrt{1+\tau^2}\sqrt{1+\frac{{\xi_y}^2}{{\xi_x}^2}\tau^2}}\,. \tag{16}$$

In Fig. 3 we show the SHG efficiencies η_g and η_{h_m}, proportional to g and h_m respectively, evaluated in the (w_{0_x}, w_{0_y}) plane for LBO crystals of lengths 9 and 23 mm. This latter one corresponds to the maximum length allowed by longitudinal walk-off when using pulses of 3 ps. We do not display the curves relative to the crystals of 13- and 17-mm lengths, since they are qualitatively very similar to the ones shown.

The grey regions in Fig. 3 indicate the parameter ranges in which the discrepancy between g and h_m, evaluated from the one-dimensional curves of Fig. 1, is expected to be larger than 30%.

The thick line is the bisector, along which one moves when using spherical lenses for focusing, as in the experiment reported here. In the third column of Fig. 3 we plot the ratio $\eta_g/\eta_{h_\mathrm{m}}$, which is shown to be very close to 1 in the region where our approximations are valid. From the plots of η_g or η_{h_m} in the (w_{0_x}, w_{0_y}) plane one sees that the enhancement of the SHG efficiency obtainable by using an elliptical rather than a spherical focusing is of the order of 20% for the three crystals considered. Although this increase may not be considered very important for many purposes, it is worth mentioning that other advantages can result from asymmetric focusing. On one hand, the optimal efficiency for elliptical focusing is obtained at much lower intensities than in the spherical focusing case. In the case that high-power lasers are used, this feature can be useful in order to avoid damage to the crystal or to the coatings. Furthermore, following the discussion about the spatial properties of the generated beam of Sect. 2, it is expected that focusing less tightly along the walk-off direction with respect to the spherical case leads to a better beam quality.

5 Conclusion

In conclusion, we have given a complete quantitative characterization of the second harmonic generated by a Ti:Sa laser operating in the ps regime, in LBO crystals of different lengths, when varying the focus of the red input beam. The above considerations of efficiency as well as transverse spatial beam parameters may be helpful in deciding which configuration is the most suitable for any given application requiring this kind of light source.

REFERENCES

1 C. Chen, Y. Wu, A. Jiang, B. Wu, G. You, R. Li, S. Lin: J. Opt. Soc. Am. B **6**, 616 (1989)
2 S. Velsko, M. Webb, L. Davis, C. Huang: IEEE J. Quantum Electron. **27**, 2182 (1991)
3 N.A. Plyneva, N.G. Kononova, A.M. Yurkin, G.G. Bazarova, V.I. Danilov: J. Cryst. Growth **198–199**, 546 (1999)
4 Y.Q. Yao, W.Q. Shi, J.E. Millerd, G.F. Xu, E. Garmire, M. Birnbaum: Opt. Lett. **15**, 1339 (1990)
5 A. Borsutzky, R. Bruenger, C. Huang, R. Wallenstein: Appl. Phys. B **52**, 55 (1991)
6 A. Nebel, R. Beigang: Opt. Lett. **16**, 1729 (1991)
7 G.A. Skrypko, S.G. Bartoshevich, I.V. Mikhnyuk, I.C. Tarazavich: Opt. Lett. **16**, 1726 (1991)
8 I.J. Evans, C.E. Webb: Opt. Commun. **113**, 72 (1994)
9 X. Liu, L. Quian, F.W. Wise: Opt. Commun. **144**, 265 (1997)
10 J. Zhang, J.Y. Huang, H. Wang, K.S. Wong, G.K. Wong: J. Opt. Soc. Am. B **15**, 200 (1998)
11 T. Kellner, F. Heine, G. Huber: Appl. Phys. B **65**, 789 (1997)
12 C.S. Adams, A.I. Ferguson: Opt. Commun. **90**, 89 (1992)
13 S. Bourzeix, M.D. Plimmer, F. Nez, L. Julien, F. Biraben: Opt. Commun. **99**, 89 (1993)
14 B. Beier, D. Woll, M. Scheidt, K.J. Boller, R. Wallenstein: Appl. Phys. Lett. **71**, 315 (1997)
15 T. Kaing, M. Houssin: Opt. Commun. **157**, 155 (1998)
16 G.D. Boyd, D.A. Kleinman: J. Appl. Phys. **39**, 3597 (1968)
17 A. Yariv: *Quantum Electronics* (Wiley, New York 1989)
18 V.G. Dmitriev, G.G. Gurzadyan, D.N. Nikogosyan: *Handbook of Nonlinear Optical Crystals* (Springer, Berlin 1990)
19 For an updated collection of bibliographic references about LBO, see e.g. the documentation enclosed with the code SNLO by A. Smith, obtainable at http://www.sandia.gov/imrl/XWEB1128/xxtal.htm
20 D.A. Kleinman, A. Ashkin, G.D. Boyd: Phys. Rev. **145**, 338 (1966)
21 F.M. Librecht, J.A. Simons: IEEE J. Quantum Electron. **11**, 850 (1975)
22 A. Steinbach, M. Rauner, F.C. Cruz, J.C. Bergquist: Opt. Commun. **123**, 207 (1996)